Noise effects in a nonlinear dynamic system: The rf superconducting quantum interference device

A. R. Bulsara and E. W. Jacobs
Naval Ocean Systems Center, Research Branch, San Diego, California 92152-5000

W. C. Schieve
Department of Physics and Center for Studies in Statistical Mechanics, University of Texas, Austin, Texas 78712
(Received 26 April 1990)

We consider the rf superconducting quantum interference device above its homoclinic threshold. The effects of weak additive (i.e., Langevin) noise on the dynamics of the system are analyzed from the standpoint of the effects on the chaotic attractors and the maximal Liapunov exponents that characterize the system in this regime. It is seen that noise has a "smoothing" effect on chaotic attractors. On the other hand, the injection of noise can lead to a change in sign of the Liapunov exponent that characterizes a periodic point in its absence, leading to "noise-induced chaos." We also consider the cases of additive fluctuations that manifest themselves as a fluctuating dc driving term, and multiplicative fluctuations (at initial times) in the nonlinearity parameter. In these cases, we study the motion of the system, in the mean, by averaging over numerous realizations of the fluctuating driving term. Depending on the strength of the fluctuations, one obtains mixtures of periodic and chaotic motion in the multiplicative-noise case.

I. INTRODUCTION

When one considers the dynamics of a nonlinear system in the real world, the presence of noise in the external perturbation cannot be ruled out. Early work on the effects of weak Langevin noise (such noise manifests itself as an additive term in the external perturbation) on simple deterministic maps was carried out by Crutchfield, Farmer, and Huberman,[1] who found that the noise introduced a gap in the period-doubling bifurcation sequence of the map; as a consequence, a scaling behavior in the characteristic exponent at the chaotic threshold was postulated. Their work complemented the investigations of Mayer-Kress and Haken.[2] Similar calculations have been carried out by Svensmark and Samuelson[3] on the Josephson junction; they found that in the presence of noise and a resonant external perturbation, the bifurcation point shifted by an amount proportional to the square of the perturbing amplitude. Wiesenfeld and McNamara[4] have investigated the amplification of a small resonant periodic perturbation in the presence of noise near the period-doubling threshold, Kautz[5] has investigated the problem of thermally induced escape from the basin of attraction in a dc-biased Josephson junction and Herzel and Ebeling[6] have investigated the effects of weak noise on the Selkov oscillator that describes glycolytic oscillations. More recently, Kapitaniak[7] has observed that the probability density function that characterizes a dissipative nonlinear system driven by random and periodic forces displays multiple maxima in the chaotic regime (such nondifferentiable probability density functions have also been postulated by Graham and Tel[8] in the chaotic regime). Finally, Lima and Pettini[9] have shown that chaotic behavior in a Duffing oscillator may be suppressed through the addition of a small parametric perturbation of appropriate frequency.

In this work, we consider a specific nonlinear dynamic system, the rf superconducting quantum interference device (SQUID). The homoclinic threshold (defined by the zero of the Melnikov function) has been computed for this system in Ref. 10. Further, the effects of *weak* Gaussian δ-correlated additive and multiplicative noise on the homoclinic threshold has been investigated by the authors.[11,12] It has been found that *on average,* additive noise elevates or postpones the homoclinic threshold. Multiplicative noise (characterized by fluctuations in the nonlinearity parameter) may either elevate or lower the homoclinic threshold depending on one's choice of the ensemble average of the velocity variable $\dot{x}(t)$ at initial times $t=0$. In this work, we consider the rf SQUID above its homoclinic threshold. The dynamics of the SQUID are reviewed below. We then consider the effects of Langevin noise on a deterministic chaotic attractor and its associated multimaximum probability density function. This is followed by a study of the effects of noise on a periodic solution; the noise induces chaoslike behavior. The behavior of the maximal Liapunov exponent in the presence of noise is analyzed in detail in this section. The case of multiplicative fluctuations (in the nonlinearity parameter) has been briefly considered; for sufficiently weak noise, the results are seen to be qualitatively similar to the additive-noise case and are not reproduced in this work. A similar result has been reported in Ref. 1, where it is shown that for a simple one-dimensional (1D) map the net effects of additive and "parametric" noise are the same for small fluctuations. Finally, we consider the special case of a random dc-driving term on the averaged dynamics of the SQUID. The results, particularly for the multiplicative-noise case (corresponding to fluctuations at time $t=0$ in the nonlinearity parameter), are seen to be quite different from the time-dependent case considered through the early

part of the paper.

In its simplest form, the rf SQUID consists of a single Josephson junction shorted by a superconducting loop of inductance L. An external magnetic field produces a geometric flux Φ_e in the loop together with a circulating current $i(t)=-I_1\sin(2\pi\Phi/\phi_0)$, where $\Phi=\Phi_e+Li$ is the actual flux sensed by the loop, with Φ_0 being the flux quantum. The flux Φ in the SQUID ring obeys the equation[13]

$$\ddot{x}+k\dot{x}+\frac{dU(x)}{dx}=\omega_0^2 x_e \ , \tag{1}$$

where

$$U(x)\equiv\frac{\omega_0^2}{2}x^2-\frac{\omega_0^2\beta}{2\pi}\cos 2\pi x \ . \tag{2}$$

Equation (1) describes a particle moving in a sinusoidally modulated parabolic potential $U(x)$. The dot denotes time differentiation, $x\equiv\Phi/\Phi_0$, $x_e\equiv\Phi_e/\Phi_0$, $\omega_0^2\equiv 1/LC$, $k\equiv 1/RC$, and $\beta\equiv LI_1/\Phi_0$. C and R are the capacitance and normal-state resistance of the loop, with I_1 being the critical current in the junction. In the absence of a dc-driving term, one obtains multivalued solutions to (1) above a critial value $\beta_c\approx 0.7325$.

The homoclinic threshold for the system (1) in the presence of a periodic driving term has been computed via the Melnikov function in Ref. 10. In this work we consider an external driving term of the form

$$x_e=q\sin\omega t+F(t) \ , \tag{3}$$

where $F(t)$ is taken to be Gaussian, δ-correlated noise, with zero mean and variance σ^2:

$$\langle F(t)\rangle=0; \quad \langle F(t)F(t+\tau)\rangle=\sigma^2\delta(\tau) \ . \tag{4}$$

Equation (1) is numerically integrated (on an Apollo DN3500 work station) using the integration algorithm of Manella and Palleschi[14] for stochastic differential equations. As a test of this algorithm, we show (Fig. 1) the results of integrating the stochastic differential equation (1) with $\beta=0$ (i.e., the harmonic oscillator) and fitting a probability density function to the resulting stationary solution $x(t)$ (the $\dot{x}$ variable is integrated out). For this problem, the stationary probability density is well known[15] and is shown on the same figure (data points). The agreement in the figure is very good. This approach must be contrasted with that of Kapitaniak,[7] who uses a Fourier decomposition of the random force into a trignometric series with uniformly distributed random phases (such a procedure has been described in the literature by Rice[16]), after which the differential equation is integrated using standard deterministic techniques. Kapitaniak appears to have used only thirty terms in the Fourier decomposition, suggesting that this number might be sufficient to provide an accurate representation of the noise for most applications of interest. In practice, however, the number of terms required to provide agreement of the kind depicted in Fig. 1 is extremely large, rendering calculations via this procedure very slow and cumbersome. The parameter set $(\beta,\omega_0^2,k,\omega)\equiv(2,1,1,2.25)$ is considered throughout this work. For this parameter

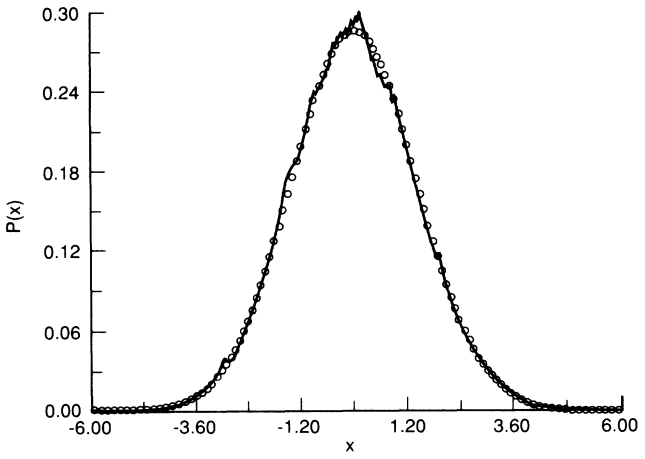

FIG. 1. Steady-state probability density function computed via integration of (1) with $\beta=0$, using algorithm of Ref. 14. The data points represent the analytic (Gaussian) probability function from Ref. 15.

set, the homoclinic threshold in the absence of noise has been found[10] to occur at $q\approx 1.25$. Throughout the rest of the work we assume the periodic driving term amplitude q to be above this value.

II. FLUCTUATIONS AND CHAOTIC DYNAMICS: "SMOOTHING" OF CHAOS

Figure 2 shows the maximal Liapunov exponent λ as a function of the periodic driving amplitude q. One observes, above the homoclinic threshold, the characteristic "windows" of periodic and chaotic behavior characterized by negative and positive values of λ, respectively. On the same figure we show the results of including additive noise of variance $\sigma^2=0.0025$ in the system dynamics. The noise has the effect of destroying the windows of periodicity (this will be discussed in Sec. III). At the same time, points that are already chaotic in the absence of the fluctuations retain the positive sign of the Liapunov exponent in the presence of noise. To gain a

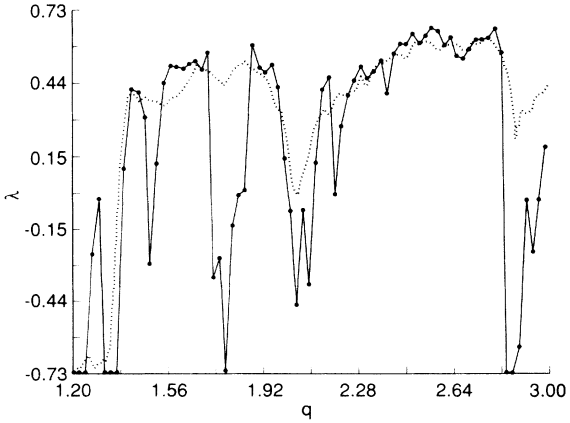

FIG. 2. Maximal Liapunov exponent λ as a function of the deterministic driving coefficient q [Eq. (3)] for Langevin noise variance $\sigma^2=0$ (solid curve) and 0.0025 (dotted curve).

deeper insight into the effects of noise on chaos, one must examine its effects on the chaotic attractors and the associated probability density functions in phase space.

Figure 3 shows a deterministic chaotic attractor obtained for the case $q=1.43$. The attractor possesses the well-known fine-structure property (shown in Fig. 4), and its power spectral density resembles that of broadband noise on which harmonics of the driving frequency $\omega=2.25$ are superimposed. In the presence of small amounts of noise, a smearing occurs in the attractor, as seen in Fig. 5; a greater area of phase space is made accessible to the system in the presence of noise and the fine-structure property is lost (Fig. 6). It is readily apparent that an arbitrary, small amount of noise will be sufficient to destroy the fine-structure property of the deterministic attractor on some small scale. The power spectral density corresponding to the variable x displays (in the absence of noise) the features characteristic of deterministic chaos: a broadband component on which are superimposed harmonics corresponding to multiples of the driving frequency ω. In the presence of additive noise the broadband floor in the spectral density is elevated, leading to a progressive washing out of the peaks corresponding to the higher harmonics of ω. Eventually, for large enough noise strengths, even the peak corresponding to the fundamental harmonic is obliterated. At this point, the system dynamics are dominated by the noise and the deterministic driving term may be ignored in the analysis. The effects of noise are also seen in the phase-space probability density function (or histogram in this case) that characterizes the variable x at long times. In the absence of noise, the probability density function $P(x)$ displays the multimaximum character suggested by Graham and Tel[8] and Jauslin[17] who postulate that, above the homoclinic threshold, the probability density function is nondifferentiable. In Fig. 7, we show the probability density function corresponding to the deterministic chaotic case together with the probability density functions in the presence of noise. These probability density functions, which correspond to the *attractors* (e.g., Figs. 3 and 5) could also be obtained by setting up and solving

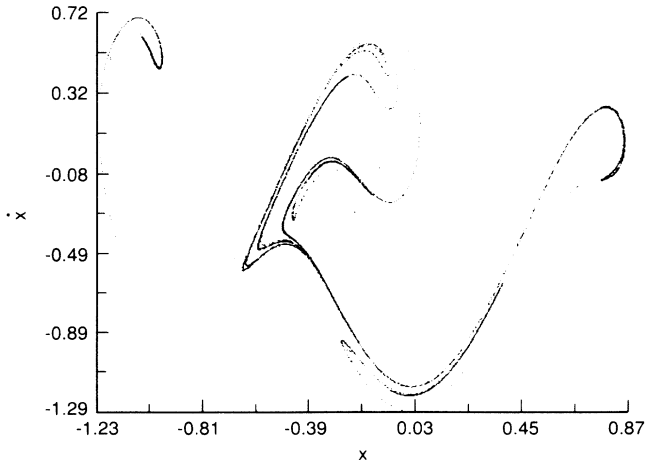

FIG. 3. Deterministic attractor in the absence of noise; $q=1.43$.

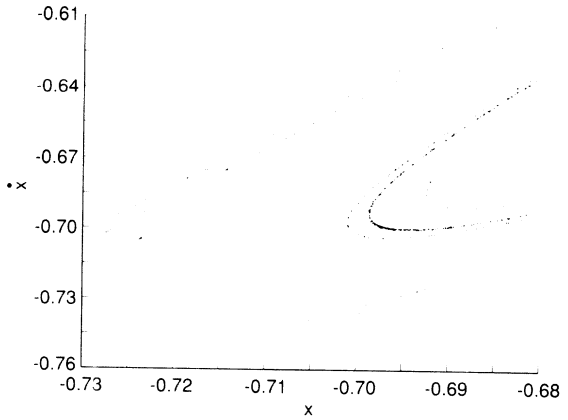

FIG. 4. Section of the attractor of Fig. 3 showing the fine-structure property.

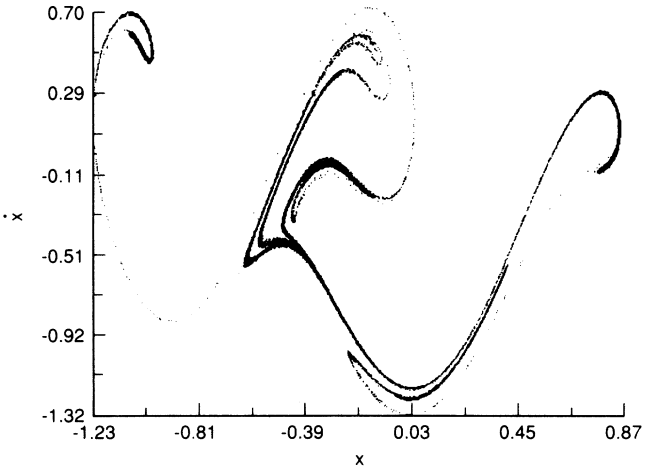

FIG. 5. Noisy chaotic attractor for $(q,\sigma^2)=(1.43,10^{-5})$.

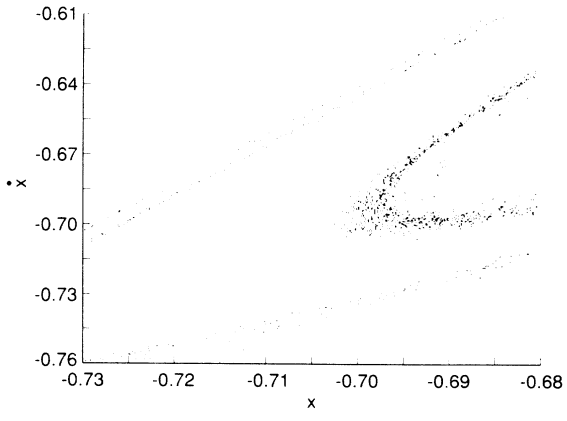

FIG. 6. Section of the attractor of Fig. 5; the fine-structure property is absent.

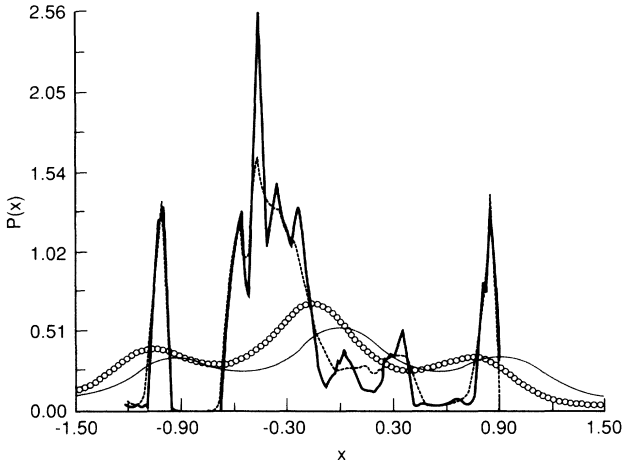

FIG. 7. Phase-space probability density function $P(x)$ for the attractors corresponding to $q=1.43$ and $\sigma^2=0$ (solid curve), 0.001 (dotted curve), and 1.0 (data points). The lower solid curve is obtained from Eq. (5) ($\sigma^2=1.0$).

the Fokker-Planck equation corresponding to the stochastic differential equation (1). The probability density function represents the frequency with which each area of phase space is traversed by the system. In the presence of noise, its peaks are seen to have a greater width but smaller height; the noise tends to "smooth" the probability density function, coarse graining the deterministic randomness of the attractor itself. This effect is a direct consequence of the greater area of phase space that is made available to the system in the presence of noise. For very large noise variances, the transitions between the different wells of the potential (2) become purely noise driven and $P(x)$ reduces to the characteristic broad distribution corresponding to this situation. In this case, we may ignore the deterministic driving term in (3) and write down a two-dimensional (2D) Fokker-Planck equation corresponding to the stochastic differential equation (1). The long-time solution of this Fokker-Planck equation (after integrating out the $\dot{x}$ variable) is[18]

$$P(x)=\exp\left[-\frac{k\omega_0^2}{2\sigma^2}\left[x^2-\frac{\beta}{\pi}\cos 2\pi x\right]\right], \tag{5}$$

up to a normalization constant. This probability density function has been plotted in Fig. 7 for $\sigma^2=1.0$. It yields a curve that fits the corresponding curve, computed via numerical integration of (1), reasonably well. One must realize that Eq. (5) is the probability density corresponding to the *orbits* $x(t)$. This explains the differences between the two bottom curves in Fig. 7 even for the relatively large noise strength $\sigma^2=1$ (recall that the numerically obtained curve corresponds to the Poincaré plot, not the orbits). As the noise strength increases, the points on the Poincaré plot fill almost the entire phase space and the distinction between the probability densities corresponding to the Poincaré plot and the orbits become increasingly tenuous. Ultimately, for very large noise strengths, one expects the probability densities obtained via the two approaches to coincide.

III. NOISE-INDUCED CHAOS

In the preceding section, we considered the effects of additive noise on a chaotic solution of the deterministic problem. As seen in Fig. 2, the maximal Liapunov exponent corresponding to a periodic solution changes sign under the influence of noise. This "noise-induced chaos" is investigated in this section. For simplicity, we consider a specific deterministic periodic solution, the case $q=1.79$ in Fig. 2. In the absence of noise, this corresponds to a period-two limit cycle. The Poincaré plot for this motion consists of two dots and the associated probability density function $P(x)$ consists of two δ-function peaks at the values of x corresponding to these dots. We now consider the effects of nonzero noise. In Fig. 8 we see that in the presence of very small amounts of noise, the motion is noisy period four, with a corresponding phase-space probability density function consisting of four noise-broadened peaks. As the noise is increased further, we obtain (Fig. 9) what appears to be a chaotic attractor. The attractor does not possess the fine-structure property of deterministic chaos and its probability density function (Fig. 10) consists of four distinct peaks with some intervening low-level structure. A closer analysis of the motion (by watching the orbits) shows that the system is driven, by the noise, between two period-two limit cycles and a chaotic attractor. This motion is extremely unstable (the Liapunov exponent is small and positive). As the noise strength is increased the two period-two limit cycles are washed out and the system spends more time on the attractor (the Liapunov exponent becomes larger and more peaks begin to appear in the probability density function at the expense of the four large peaks in Fig. 10). Ultimately, for very large noise, the effects of the deterministic driving may be ignored, and the probability density function resembles the third curve in Fig. 7. Once again, the effects of noise are manifest at the level of the power spectral density corresponding to x. In the absence of any noise, the spectral density consists of well-defined peaks located at multiples of $\omega/4\pi$ (Fig. 11). As the noise level is increased, the broadband floor in the

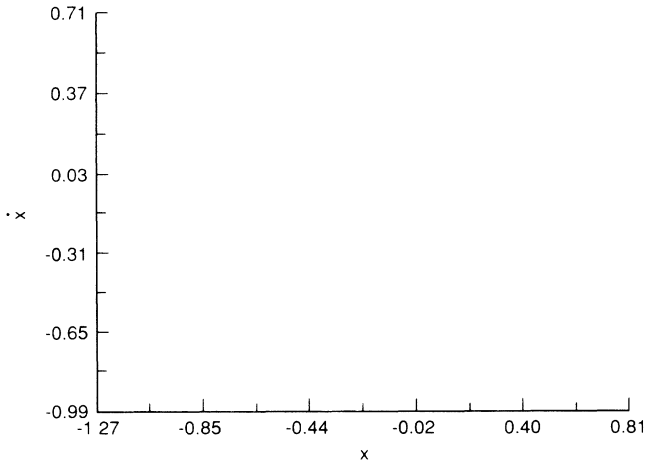

FIG. 8. Poincaré plot showing the effects of noise ($\sigma^2=10^{-5}$) on initially period-two motion ($q=1.79$). The motion is noisy period four.

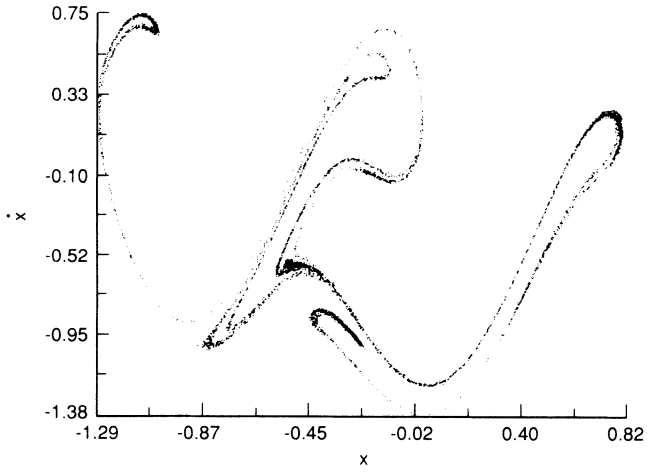

FIG. 9. Same as Fig. 8 with $\sigma^2=5\times10^{-5}$; the motion is driven between two period-two limit cycles and a chaotic attractor, by the noise.

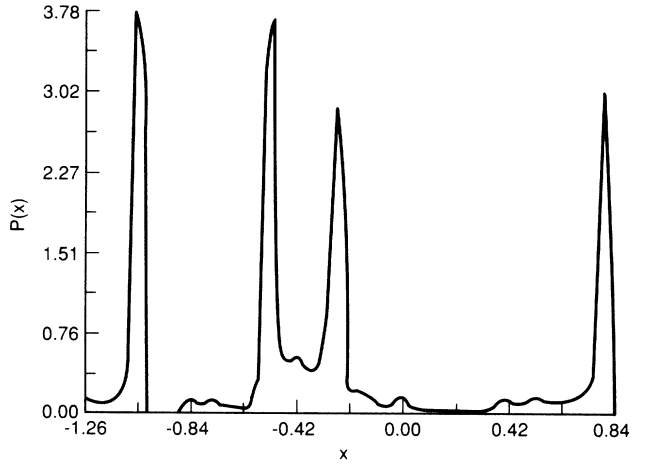

FIG. 10. Phase-space probability density function corresponding to the attractor of Fig. 9.

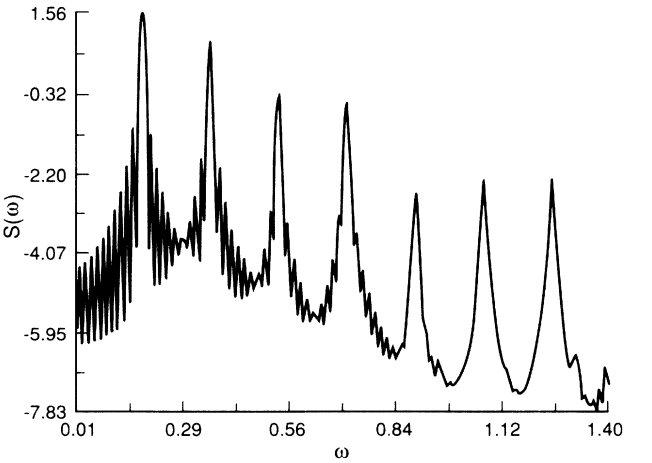

FIG. 11. Power spectral density corresponding to the variable x for $(q,\omega,\sigma^2)=(1.79,2.25,0.0)$. The peaks occur at multiples of $\omega/4\pi$.

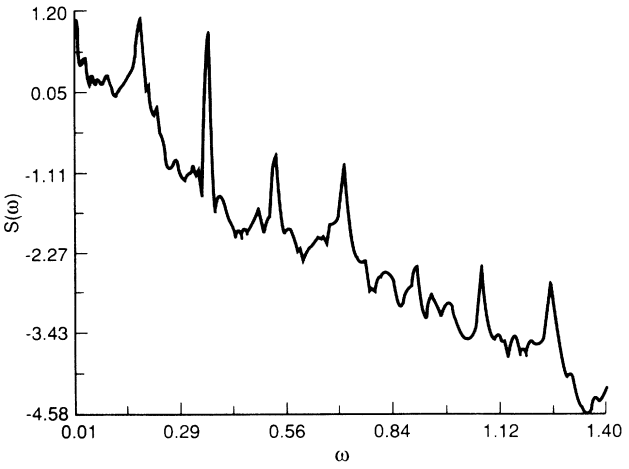

FIG. 12. Same as Fig. 11 with $\sigma^2=5\times10^{-5}$.

spectral density rises (Fig. 12), eventually obscuring the peaks for large enough noise strengths; in this limit, the spectral density resembles that which characterizes deterministic chaos.

The preceding paragraph indicates that even weak Langevin noise may introduce chaoslike behavior in a system that is periodic in the deterministic case. Such behavior occurs for all the points for which the Liapunov exponent in Fig. 2 is negative in the absence of noise. The behavior of the maximal Liapunov exponent as a function of noise strength for a given set of system and deterministic driving parameters is shown in Fig. 13 for three different values of the parameter q. Evidently there exists, for a given set of system and driving parameters, a critical noise strength σ_c^2 at which the Liapunov exponent vanishes; this critical noise strength is analogous to an order parameter if we treat the change in sign of the Liapunov exponent as a phase transition. In Fig. 14 we show values of $(\ln\sigma_c^2)/\lambda_0$ (λ_0 is the Liapunov exponent in the absence of noise) for q values corresponding to the *minimum* of the corresponding window of periodicity in Fig. 2. Hence, the value of σ_c^2 corresponding to each q

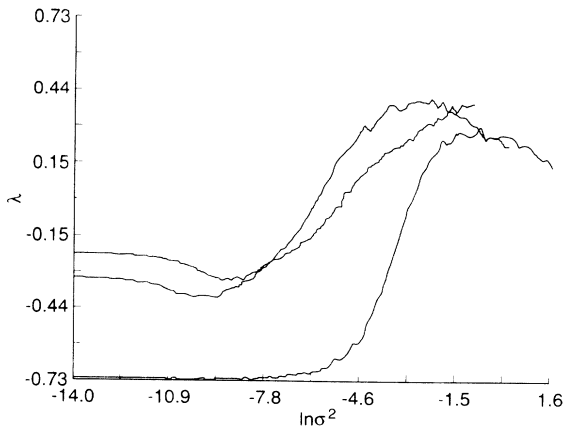

FIG. 13. Maximal Liapunov exponent λ vs $\ln\sigma^2$ for $q=5.35$ (bottom curve), 4.001 (middle curve), and 2.05 (top curve).

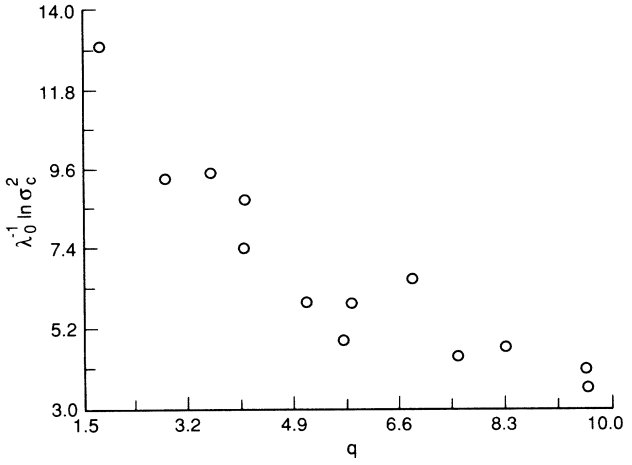

FIG. 14. $\lambda_0^{-1}\ln\sigma_c^2$ vs periodic driving parameter q. σ_c^2 is the critical noise variance at which the Liapunov exponent is zero, λ_0 being the Liapunov exponent in the absence of noise.

represents the minimum noise that completely erases this window. In connection with Figs. 13 and 14 we must point out that the dynamics in the parameter range near the zero of the Liapunov exponent are very unstable and time consuming. Hence, the quantitative results in this parameter range become dependent on the numerical algorithm used to integrate the stochastic differential equation (1).

IV. THE CASE OF RANDOM dc DRIVING TERMS

In the preceding sections we have considered the case of a time-dependent Gaussian δ-correlated noise term defined in Eq. (4). We now consider the case when $F(t)$ is a constant (i.e., dc) perturbation that fluctuates about some mean value (taken to be zero in this work) with variance σ^2. In this case, the calculations of the preceding sections must be modified. Instead of integrating the nonlinear differential equation continuously over time for very long times, we now generate a particular realization of the dc term and then integrate the differential equation (1) up to a certain final time (the final time is selected after allowing the transients to decay). We then select a new realization of F (with the same variance as before) and integrate up to the same time once again. This is repeated for 40 000 realizations of the random dc term F. It is evident that, since the dc term is kept constant throughout each integration (it takes on a new value only at $t=0$ in each of the 40 000 integrations), we are effectively solving a deterministic problem 40 000 times. For each of the realizations of the noise, we start the system at the right end point of the separatrix. This end point is recalculated for each different realization of the force. Hence, we are effectively changing the potential (2) for each of the 40 000 solutions and the Poincaré plots are obtained by plotting $\dot{x}(t_f)$ versus $x(t_f)$, t_f being the final time (an integer multiple of the Poincaré period) used in the integrations. The results for the case of additive noise acting on an initially chaotic solution are qualitatively the same as those obtained in Sec. I. Each realization of the noise, (i.e., each realization of the potential) leads to a slightly different region of phase space that is accessible to the system. Accordingly, in the presence of small amounts of additive noise, one obtains maps that are similar to the original (noise-free) attractor. The probability density functions corresponding to these noisy attractors display the same properties as those shown in Fig. 7; increasing the noise strength tends to smooth and broaden the probability density function. This case has been discussed in detail in Ref. 11 and will not be addressed further in this work. Before concluding this paragraph, one must point out that, unlike the situation of the preceding section, a solution that is initially (in the absence of noise) periodic, does *not* become chaotic in the presence of the fluctuations in the dc-driving term, as considered in this section, unless the variance of these fluctuations is very large. In the latter case there exists the possibility that a few realizations of the dc-driving term (and, hence, of the potential) may lead to chaos. For moderate variances in the fluctuations of the dc-driving term (we reiterate that we are assuming a mean value of zero), however, we usually obtain noisy periodicity, characterized by fuzziness surrounding the discrete points that make up the Poincaré plot in the absence of noise, accompanied by a broadening in the δ-function peaks comprising the noise-free probability density function. This case is to be contrasted with the effects of time-dependent additive fluctuations discussed in the preceding section.

We now consider the case of dc-multiplicative fluctuations. Specifically, the nonlinearity parameter β in (2) is assumed to fluctuate about some mean value with variance σ_M^2. Once again, we assume that the fluctuations cause the parameter to change its value at time $t=0$ only. The stochastic differential equation is integrated as described in the preceding paragraph. We find that, unlike the situation discussed in the preceding paragraph, initial time fluctuations in the nonlinearity parameter β may induce chaoslike behavior in the system. Further, a computation of the maximal Liapunov exponent for this case yields interesting behavior. At very low noise values, the Liapunov exponent (which may be treated as a random variable) displays a monomodal probability density function centered at some negative mean value. As the multiplicative noise strength is increased the probability density $P(\lambda)$ develops a second peak centered about some positive value of λ. The positive peak grows at the expense of the negative peak until a certain critical value of the noise variance at which point the reverse effect occurs: the negative peak grows as the positive peak decreases in height. These effects are summed up in Fig. 15 for the $q=1.79$ case. The explanation of this behavior is obvious. Changes in the nonlinearity parameter β can induce chaos in the system. When the differential equation (2) is integrated for 40 000 realizations of β (with β changing only at the start of each integration), it is evident that some of the β values generated by the random-number generator will be such that they support chaos in the deterministic problem (all other system and driving parameters remaining fixed), whereas other values of β will not be able to support chaos. The result is a combination of periodic and chaotic motions for a given strength of the multiplicative fluctuations. The relative heights of

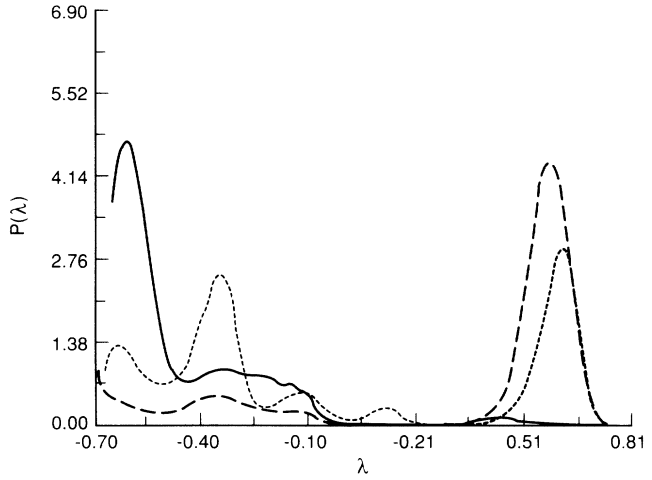

FIG. 15. Probability density function describing the Liapunov exponent for the case of initial time fluctuations in the nonlinearity β. Curves correspond to $q=1.79$ and multiplicative noise variance $\sigma_M^2=10^{-5}$ (solid), 0.0005 (dotted), and 0.05 (dashed).

the maxima in the probability density functions of Fig. 15 are an indication of which motion is preponderant *in the mean* for a given noise strength. One cannot distinguish the motions at the level of the Poincaré plot; even if chaos occurs for only a few realizations of β it would be sufficient to obscure the periodic points on the attractor. Obviously, it is meaningless, for this case to define a single-averaged Liapunov exponent λ. The probability density function corresponding to the random variable x reflects the effects described above. For a multiplicative noise strength $\sigma_M^2=10^{-6}$ it consists of four well-separated peaks with a very small amount of intervening structure. Depending on the particular realization of the parameter β, the motion can exist in one of two stable period-two limit cycles (recall that, in the absence of any noise the motion is period two) and, for only a few realizations of β, we might obtain a deterministic attractor. This case correlates with the solid curve of Fig. 15, which is characteristic of mostly periodic motion. For this case, the Poincaré plot of $\dot{x}$ vs x resembles the noisy attractor of Fig. 9. As the noise strength increases, the Poincaré plot becomes fuzzier (as seen in the preceding sections). For $\sigma_M^2=0.0005$ the probability density function $P(x)$ is still made up of four major peaks, but the intervening structure is now far more pronounced at the expense of the peak heights. This corresponds to the dotted curve in Fig. 15, which is seen to indicate a coexistence of periodic and chaotic motions. As the noise strength increases still further, the probability density function $P(x)$ becomes broader and develops still more structure, indicating that the chaotic behavior occurs more readily than the periodic behavior. This case is represented by the $\sigma_M^2=0.05$ curve in Fig. 15. We note that allowing both multiplicative and additive fluctuations simultaneously (β as well as the external dc-driving term F fluctuate but without mutual correlations) does not change, qualitatively, the results of this paragraph; the additive fluctuations simply lead to a broadening of the peaks in the probability density function $P(x)$ but do not change the system behavior as pointed out in the preceding paragraph.

V. DISCUSSION

In this work we have discussed, numerically, the effects of Langevin noise on a nonlinear dynamic system above its homoclinic threshold. This work extends the earlier work of Crutchfield *et al.*[1] on the 1D logistic map (this work is actually more analogous to the work of Herzel and Ebeling,[6] who also considered the effects of weak noise on a system described by a nonlinear differential equation), and complements our earlier work[11,12] on the effects of *weak* additive and multiplicative noise on the homoclinic threshold as defined by the zeros of the Melnikov function. We find that weak Langevin noise leads to a "smoothing" of chaos: the deterministic attractor occupies a greater region of phase space and the corresponding probability density function is smoother and broader. The noise actually enhances the observability of the chaos. Further, if we start with a point that is periodic in the absence of noise, the noise leads ultimately to chaoslike behavior (so-called "noise-induced chaos") characterized by a positive Liapunov exponent. As seen from our example of Sec. III, however, one must take care in the interpretation of these results; what appears to be a chaotic attractor in Fig. 9 is actually a coexistence of two period-two motions and a chaotic attractor with only a relatively small amount of time spent on the attractor. This motion is quite unstable (the Liapunov exponent is approximately 0.03) and, for larger amounts of noise, it settles down on the attractor (the Liapunov exponent becomes larger). The phase-space probability density function (Fig. 10) reflects the above statements. The case of multiplicative fluctuations (in β) was examined. However, the results (at least for weak-to-moderate noise) were found to be qualitatively similar to those for additive noise. This has also been shown by Crutchfield, Farmer, and Huberman.[1] It is important to point out that whereas noise produces chaoslike behavior out of periodic motion, the reverse process does not occur: large amounts of noise will not lead to higher-order periodicity when applied to any of the points on Fig. 2 (solid curve) for which the Liapunov exponent is initially positive.

The case of having noise present as a random dc input has been briefly considered. Such noise often occurs as a natural part of the measurement process when one is faced with system (e.g., circuit, in this case) or external parameters that do not remain constant but fluctuate about some average values. If the measurement time is less than or comparable to the critical time scale of the fluctuations, then the results of Sec. IV might be expected to provide a good insight into the mean behavior of the system. The case of $F(t)$ in Eq. (3) being colored noise with extremely long correlation time also falls within this category. In this case, the additive fluctuations lead to a broadening of the deterministic chaotic attractor similar to the effects observed in the example of Sec. II. The multimaximum probability density function associated with the deterministic chaotic attractor also undergoes a

smoothing in the presence of the fluctuations, with more regions of phase space becoming accessible to the system. It is worth pointing out that one may further quantify the effects of noise on the probability density by computing the information dimension defined as[19]

$$d_I = \frac{\sum_{i=1}^{N(\epsilon)} P_i \ln P_i^{-1}}{\ln \epsilon^{-1}} , \tag{6}$$

in the $\epsilon \rightarrow 0$ limit, where $N(\epsilon)$ represents the number of squares of side ϵ necessary to cover the attractor, and P_i the relative probability of each square being visited. In the absence of noise, a relatively small area of phase space is accessible to the system (corresponding to the deterministic chaotic attractor of Fig. 3 and the associated probability density function indicated by the solid curve in Fig. 7) and the information capacity of the deterministic attractor is found to be approximately 1.18. As the noise strength is increased, however, more regions of phase space become accessible to the system and the information dimension increases. The information capacity may also be calculated, in a similar manner, for the case of the time-dependent fluctuations considered in the preceding section. All calculations of the information capacity in the presence of noise suffer, however, from the basic drawback of a paucity of points at low box dimensions [a plot of $\ln N(\epsilon)$ versus $\ln \epsilon^{-1}$ begins to level off at large values of ϵ^{-1}]. Hence, these calculations yield acceptable results only when one can generate attractors with huge numbers of points, a process that is extremely time consuming. Further, when a formula of the form (6) is used to calculate d_I, one assumes that the graph of $\sum_{i=1}^{N(\epsilon)} P_i \ln P_i^{-1}$ versus $\ln \epsilon^{-1}$ is approximately linear (until the box dimension ϵ becomes very small) so that d_I may be calculated from the slope of this straight line. Such a situation occurs, in fact for deterministic chaotic attractors; however, in the presence of noise, the linear regime of these plots is extremely small, thereby introducing a further element of unreliability into the calculation.

It has been pointed out that, unlike the case discussed in Sec. III, fluctuations in the dc-driving term do not (for moderate noise strengths) produce chaos out of initially periodic solutions. Multiplicative noise (acting at initial times) on the other hand produces effects similar to those discussed in Sec. III: it produces mixtures of periodic and chaotic behavior depending on the variance of the fluctuations. Such behavior might be expected on purely physical grounds since it is well known that small changes in the nonlinearity parameter β can trigger chaos. As in the case of time-dependent fluctuations discussed in Sec. III, the system, depending on the particular realization of the multiplicative noise, can lie on a limit cycle or a chaotic attractor. The net motion, averaged over all the realizations of the noise, is characterized by a bimodal probability function for the Liapunov exponent. The relative heights of the peaks may be used as a measure of the frequency of each type of motion.

ACKNOWLEDGMENTS

A.R.B. would like to acknowledge support from the Office of Naval Research under Grant No. N0001490AF00001, as well as numerous useful discussions with Dr. P. Jung (University of Augsburg, Federal Republic of Germany).

[1]J. Crutchfield, J. D. Farmer, and B. Huberman, Phys. Rep. **92**, 45 (1982).
[2]G. Mayer-Kress and H. Haken, J. Stat. Phys. **26**, 149 (1981).
[3]H. Svensmark and M. Samuelson, Phys. Rev. A **36**, 2413 (1987).
[4]K. Wiesenfeld and B. McNamara, Phys. Rev. Lett. **55**, 10 (1985).
[5]R. Kautz, Phys. Rev. A **38**, 2066 (1988).
[6]H. Herzel and W. Ebeling, Z. Naturforsch **42A**, 136 (1987).
[7]T. Kapitaniak, *Chaos in Systems with Noise* (World Scientific, New York, 1988).
[8]R. Graham and T. Tel, J. Stat. Phys. **35**, 729 (1984).
[9]R. Lima and M. Pettini, Phys. Rev. A **41**, 726 (1990).
[10]W. C. Schieve, A. R. Bulsara, and E. W. Jacobs, Phys. Rev. A **37**, 3541 (1988).
[11]A. R. Bulsara, W. C. Schieve, and E. W. Jacobs, Phys. Rev. A **41**, 668 (1990).
[12]W. C. Schieve and A. R. Bulsara, Phys. Rev. A **41**, 1172 (1990).
[13]R. Barone and G. Paterno, *Physics and Applications of the Josephson Effect* (Wiley, New York, 1982).
[14]R. Manella and V. Palleschi, Phys. Rev. A **40**, 3381 (1989)..
[15]M. Wang and G. Uhlenbeck, in *Selected Papers on Noise and Stochastic Processes,* edited by N. Wax (Dover, New York, 1954), p. 113.
[16]S. O. Rice, Ref. 15, p. 133.
[17]H. Jauslin, J. Stat. Phys. **42**, 573 (1986).
[18]A. R. Bulsara, J. Appl. Phys. **60**, 2462 (1986).
[19]J. D. Farmer, E. Ott, and J. Yorke, Physica D **7**, 153 (1983).